Nanodroplet-based reagent delivery into water-in-fluorinated-oil droplets

Bo Zhu, * ‡ [a, b, c] Zhe Du, ‡ [b, d] Yancen Dai, [c] Tetsuya Kitaguchi, [c] Sebastian Behrens [b, e] and Burckhard Seelig * [a, b]

[a] Department of Biochemistry, Molecular Biology and Biophysics, University of Minnesota, Minneapolis, MN 55455, USA.

[b] BioTechnology Institute, University of Minnesota, St. Paul, MN 55108, USA.

[c] Laboratory for Chemistry and Life Science, Institute of Innovative Research, Tokyo Institute of Technology, Yokohama, Kanagawa 226-8503, Japan.

[d] Center for Environmental Health Risk Assessment and Research, Chinese Research Academy of Environmental Sciences, Beijing 100012, China.

[e] Department of Civil, Environmental, and Geo- Engineering, University of Minnesota, Minneapolis, MN 55455, USA.

‡ Contributed equally to this work.

***Correspondence:**

Bo Zhu

zhu.b.ac@m.titech.ac.jp

Burckhard Seelig

seelig@umn.edu

Abstract

In vitro compartmentalization is a technique for generating water-in-oil microdroplets to establish the genotype (DNA information)-phenotype (biomolecule function) linkage required by many biological applications. Recently, fluorinated oils have become more widely used for making microdroplets due to their better biocompatibility. However, it is difficult to perform multi-step reactions requiring the addition of reagents in water-in-fluorinated-oil microdroplets. On-chip droplet manipulation is usually used for such purposes, but it may encounter some technical issues of low throughput or time delay of reagent delivery into different microdroplets. Hence, we evaluated the feasibility of employing a nanodroplet-based approach to address these issues using copper ions and a middle-size peptide (2 kDa) molecule.

Introduction

In vitro compartmentalization (IVC) was first developed by Dan Tawfik and Andrew Griffiths in 1998 for high-throughput directed evolution.[1] Through this approach, a genotype-phenotype linkage is achieved due to a physical barrier provided by artificial reaction compartments such as water-in-oil droplets, which mimic the cells of living organisms. Currently, IVC-based methods have been already used to perform various biological applications including evolving enzymes[1-8], prototyping genetic circuits[9], and screening high secretion cell strains[10]. Among these methods, the uniform water-in-oil microdroplets generated by microfluidic devices have become more popular in recent years because they can achieve the often desired single molecule/cell encapsulation.[11] Regarding the required chemicals, fluorinated oils have been more widely used for producing microfluidic microdroplets since 2000.[12, 13] Together with well-designed surfactants, fluorinated oils are more biocompatible and stable than hydrocarbon oils (e.g., mineral oil, hexadecane), because fluorinated oils are immiscible with either water or hydrocarbons (lipids).[12, 14, 15]

Many cellular and biochemical assays involve multi-step reactions requiring the addition of certain reagents or chemicals (i.e., Cu^{2+} or other metal ions), for example, to start or terminate reactions, lyse cells, facilitate, or disrupt protein folding, etc. Microdroplet systems are compatible for reagent delivery during multi-step reactions in principle. On-chip droplet manipulation is currently the main approach to achieve such purposes, including picoinjection[9] and droplet fusion[13]. However, it remains challenging to perform these droplet manipulation-based methods, since they usually require specialized microfluidic devices or advanced electric field control, which are not easily accessible to many users. In addition, droplet manipulation-based approaches often have some technical issues, such as low throughput and time delay of reagent delivery among different microdroplets.

A nanodroplet-based reagent delivery is a simple and promising alternative that does not require any complicated setups. Theoretically, it can enable the simultaneous reagent delivery into entire batches of microdroplets, to trigger or inhibit targeting cellular and biochemical assays. Furthermore, this approach can accomplish high-throughput reagent delivery without changing the droplet volume significantly in general. The nanodroplet-based reagent delivery so far has only been used to add metal ions in water-in-mineral-oil microdroplets generated using bulk methods.[4] It has not been well assessed yet whether the delivery of metal ions or middle-size biomolecules into water-in-fluorinated-oil microdroplets works using nanodroplets, which both are common reagents for multi-step cellular and biochemical reactions.

In this study, we performed copper ions and a 20 amino acid human p53 peptide delivery into water-in-fluorinated-oil droplets via nanodroplets. We confirmed the delivery of copper ions by microscopic inspection of $Cu(OH)_2$ crystal formation on pre-encapsulated iron oxide-containing microbeads under alkaline condition[16]. Similarly, we also confirmed the delivery of the 20 amino acid human p53 peptide by visualizing the fluorescent signals in water-in-fluorinated-oil microdroplets containing the p53 fluorescent immunosensor.[17] We revealed that the nanodroplet-based reagents delivery was a promising approach for metal ions and middle-size biomolecules delivery into water-in-fluorinated-oil microdroplets. It has a great potential to be used for performing multi-step cellular and biochemical

assays within water-in-fluorinated-oil microdroplets such as synchronously triggering the alkyne-azide click reaction[18, 19], activation of enzymes[20, 21], or the inhibition of enzymatic reactions[22, 23] in water-in-fluoronated-oil droplets.

Results and Discussion

The water-in-fluorinated-oil microdroplets were prepared by the flow-focusing method[9] on a 30 µm microfluidic chip (**Fig. 1A**). The dispersed and continuous phases were microbeads-suspended alkaline buffer and HFE-7500 fluorinated oil with 2% Pico-Surf 1 surfactant, respectively. The average size of the microdroplets was 22.1 µm in diameter with a 4% coefficient of variation (CV) (**Fig. 1B**).

The copper ion nanodroplets were prepared by emulsifying 1 µL of copper sulfate solution in a 250 µL of fluorinated oil containing the same surfactant (**Fig. 1C**). The size of the nanodroplets was determined by dynamic light scattering (DLS) (**Fig. 1D**). The nanodroplets had a mean volume diameter of 10.4 ± 2.6 nm, which falls in the common range of 10–200 nm reported in previous studies.[18, 19]

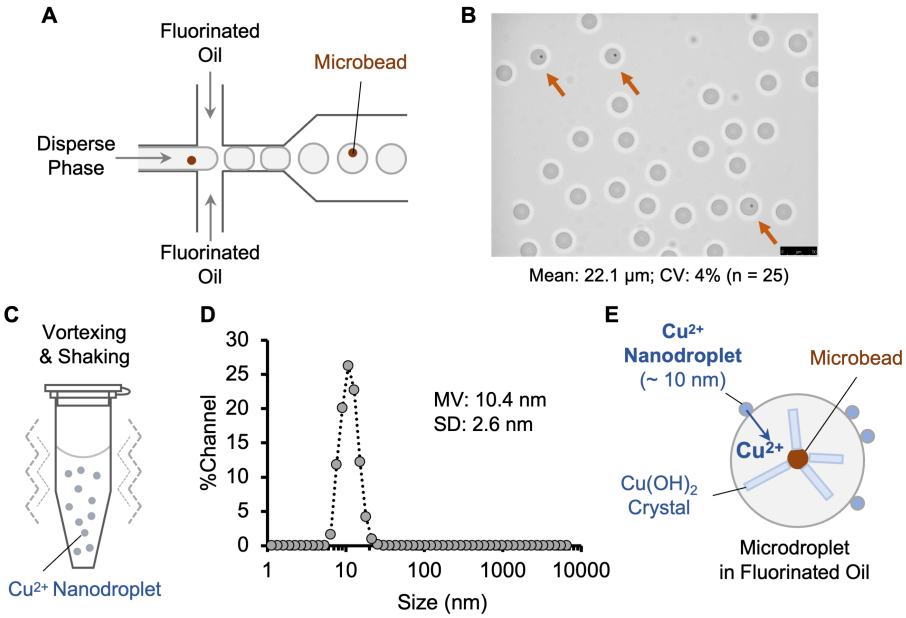

Fig. 1. Copper ion delivery into water-in-fluorinated-oil droplets via nanodroplets. (A) Generation of uniform water-in-fluorinated-oil microdroplets by flow-focusing microfluidic device. (B) Microscopy image of microdroplets. Red arrows indicate the microdroplets containing a microbead. Scale bar, 25 µm. CV: coefficient of variation. (C) Preparation of copper ion nanodroplets by vortexing. (D) Size distribution of the copper ion nanodroplets analyzed by dynamic light scattering. MV: mean volume diameter. SD: standard deviation. (E) Delivery of copper ions into microdroplets through co-incubation and crystal formed on microbeads confirming successful delivery to copper ions.

Nanodroplet size can be influenced by several factors, including relative viscosity, surfactant concentration, surfactant length, and vortex time.[20, 22] The low-energy methods such as vortexing and manual shaking usually generate smaller nanodroplets compared to high-energy methods of sonication and high-pressure homogenization.[20]

The copper ion delivery (**Fig. 1E**) was achieved by simply mixing the nanodroplet and microdroplet solutions at a 1:1 volume ratio. The emulsion mixture was gently inverted 5 times and incubated in the dark as recommended by the manufacturer of the surfactant and oil. The emulsion mixture was visualized with a microscope after 19 h (**Fig. 2A-C**) and 45 h of incubation (**Fig. 2D-F**). The clear crystals formed on the microbeads was observed after 19 h incubation with copper ion nanodroplets, which proved the successful delivery of copper ions into the water-in-fluorinated-oil droplets. The crystals were more evident after 45 h incubation. However, a size change of the microdroplets was observed after incubation with nanodroplets for both 19 and 45 h, which could be due to crystal- and nanodroplets-mediated

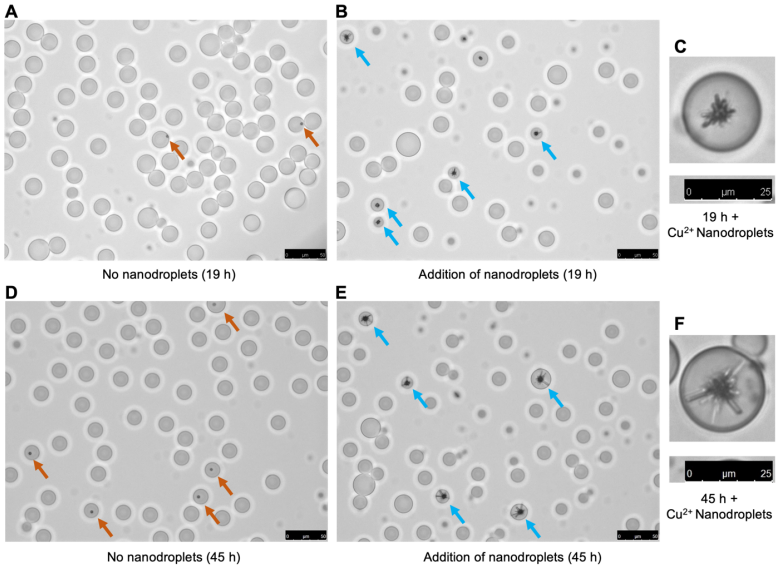

Fig. 2. Confirmation of the copper ion delivery into water-in-fluorinated-oil microdroplets via crystal growth on microbeads. (A) 19 h incubation in the absence of copper nanodroplets, 20× objective lens. (B) 19 h incubation in the presence of copper nanodroplets, 20× objective lens. (C) cropped single microdroplet image after 19 h incubation in the presence of copper nanodroplets, 40× objective lens. (D) 45 h incubation in the absence of copper nanodroplets, 20× objective lens. (E) 45 h incubation in the presence of copper nanodroplets, 20× objective lens. (F) cropped single microdroplet image after 45 h incubation in the presence of copper nanodroplets, 40× objective lens. Red arrows indicate the microdroplets containing microbeads under the control condition. Blue arrows indicate the droplets showing crystal formed on microbeads. 20× objective lens scale bar, 50 μm; 40× objective lens scale bar, 25 μm.

droplet coalescence. Overall, we demonstrated that it is applicable to deliver metal ions into water-in-fluorinated-oil microdroplets using nanodroplets. Furthermore, the label-free approach we used to confirm copper ion delivery into water-in-oil microdroplets could potentially be adapted and used in combination with other metal ions and crystal formation conditions.

Similar protocol was performed to verify a middle-size biomolecule of 20 amino acid human p53 peptide delivery into water-in-fluorinated-oil microdroplets using nanodroplets (**Fig. 3A**). The dispersed phase containing the human p53 protein fluorescent immunosensor (p53 Quenchbody) was used to make microdroplets for reagent delivery assessment of middle-size biomolecules.[17] The sensor microdroplets were defined as the ones containing the p53 Quenchbody but without p53 peptide, which had low

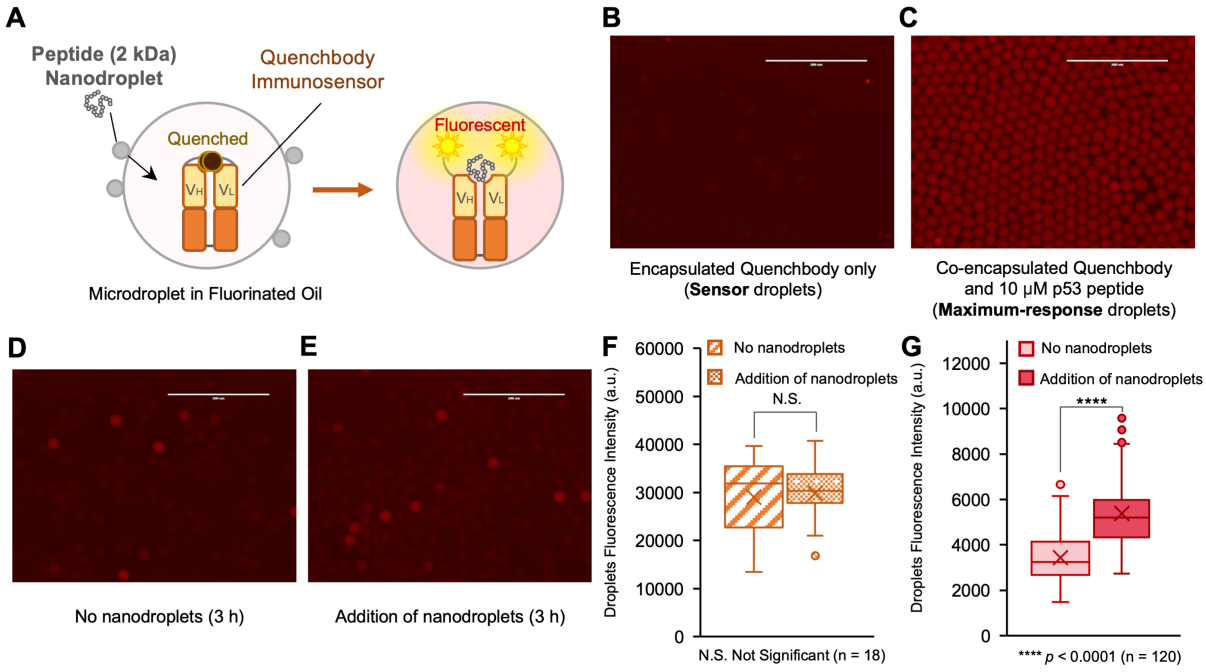

Fig. 3. Nanodroplet-based peptide delivery into water-in-fluorinated-oil microdroplets. (A) Scheme of nanodroplet-based peptide delivery and visualization by immunosensor (Quenchbody). V_H and V_L, variable region of heavy chain and light chain of antibody. (B) Microdroplets containing Quenchboday only (sensor droplets). (C) Microdroplets containing both Quenchbody and 10 μM human p53 peptide (maximum-response droplets). The maximum-response droplets are spiked into the sensor droplets as internal control during fluorescence imaging. (D) Incubation of mixed microdroplets (90% sensor droplets and 10% maximum-response droplets) in absence of nanodroplets after 3 h. (E) Incubation of mixed microdroplets with p53 peptide-containing nanodroplets after 3 h. Scale bar, 200 μm. (F) Box plot of fluorescence intensity of the maximum-response droplets after 3 h incubation. (G) Box plot of fluorescence intensity of sensor droplets after 3 h incubation. Box plots indicate the median (centre line), mean (cross), first and third quartiles (box edges) and full data ranges (whiskers), and outlier (circles). The level of significance was determined by two-tailed Welch's *t*-test.

background fluorescence intensity **(Fig. 3B)**. When p53 Quenchbody binds to the human p53 peptide, the complex will yield strong fluorescence. The maximum response microdroplets (positive control) were prepared by encapsulating both Quenchbody and peptide. Due to the elevated concentration of the human p53 peptide encapsulated in positive control microdroplets, they showed much stronger (over 10-fold) fluorescence intensity than sensor microdroplets (**Fig. 3C**). The mean diameter of the microdroplets was 21.5 μm (CV 6%). Before spiking nanodroplets into microdroplets for the human p53 peptide delivery, positive control microdroplets were mixed with sensor microdroplets in a ratio of 1:9, which served as internal controls for fluorescence intensity comparison among different samples or microscopic image analysis. The microdroplet mixture was incubated with/without nanodroplets in dark for 3 h to evaluate the human p53 peptide delivery. The microscopy images of both samples were shown in **Fig. 3D** and **3E**, respectively. After incubation, all bright red microdroplets were the positive control ones showing the fluorescence intensity larger than 10,000 (a.u.). The addition of nanodroplets didn't cause a significant change in fluorescence intensity of the positive control (max-response) microdroplets (**Fig. 3F**). A 1.6-fold increase in fluorescence intensity was observed in remaining sensor microdroplets (**Fig. 3G**). It demonstrates the successful human p53 peptide delivery in sensor microdroplets. The average human p53 peptide concentration within microdroplets was further estimated as 28 nM according to a dose-response curve measured in bulk condition (**Fig. S1**). The human p53 peptide delivery into sensor microdroplets by nanodroplets was also performed using a longer incubation time of 24 h. It could only result in a 1.8-fold increase of fluorescence intensity (equivalent to 34 nM in concentration) (**Fig. S2**), which suggested that the human p53 peptide delivery was the most efficient in the first 3 h. This result revealed the feasibility of using nanodroplets to achieve middle-size biomolecule delivery into water-in-fluorinated-oil microdroplets.

Recently, a sodium dodecyl sulfate (SDS)-triggered cargo release approach was reported for synchronized reagent delivery in microdroplets to achieve multi-step bioassays in a water-in-oil-in-water double emulsion (DEs) system. Furthermore, liposome cargos containing the reaction reagents needed

to be co-encapsulated in the aqueous core of DEs.[24] Briefly, after the addition of SDS in outer aqueous phase, a certain amount of SDS would diffuse into the aqueous core of DEs to lyse the liposomes and release the inner contents. So, the corresponding bioassays could be triggered at a desired time point. This method is suitable for relatively hydrophilic or large molecules but is not compatible with phospholipid membrane-permeable compounds due to the characteristics of liposomes. And the biochemistry assay in the DEs must be tolerant to the ionic surfactant SDS. The nanodroplet-based reagent delivery method described in this study can be a relatively straightforward alternative to achieve the same goal of performing muti-step bioassays without introducing the additional trigger molecues (e.g. SDS) in water-in-oil microdroplets or two-step DE generation system[9]. In the future, the systematic evaluation of the effects of surfactant concentration, size of droplet, and molecular weight of the reagents to be delivered could be performed with the methods provided in this study to have a deeper understanding of the mechanism and limitation of the nanodroplet-based reagent delivery.

Conclusions

In conclusion, we demonstrated that nanodroplets could be used as carriers for metal ions and middle-size biomolecule (2 kDa peptide) delivery into water-in-fluorinated-oil microdroplets. This straightforward nanodroplet preparation and delivery procedure without the need of specialized equipment or complicated setup make it easy to access for many researchers. We believe that this nanodroplet-based delivery method is a promising approach capable of achieving multi-step cellular and biochemical assays in artificial reaction compartments for a broad range of biological applications, including molecular evolution, cell factory engineering, or drug screening.

Materials and Methods

Materials. Pico-Surf 1 was purchased from Sphere Fluidics (Cambridge, UK). HFE 7500 fluorocarbon oil was purchased from 3M (Maplewood, MN, USA). FluoSurf (2%, w/w) in HFE 7500 was purchased from Emulseo (Pessac, France). Dynabeads M-270 Epoxy was purchased from Thermo Fisher Scientific (Waltham, MA, USA). Other chemicals used in this study were purchased from Sigma-

Aldrich (St. Louis, MO, USA) unless stated otherwise. The 30 μm microfluidic chip was purchased from Dolomite Microfluidics, a brand of Blacktrace Holdings Ltd (Royston, UK). The 20 μm microfluidic chip (Fluidic 947, Topas) was purchased from microfluidic ChipShop (Jena, Germany).

Preparation of copper ion nanodroplets. To encapsulate the copper ions into nanodroplets, 1 μL of 250 mM $CuSO_4$ solution was added into 250 μL HFE 7500 fluorinated oil containing 2% (w/w) Pico-Surf 1 surfactant. The mixture was then emulsified by vortexing three times at the maximum speed for 1 min with a Vortex-Genie 2 (Scientific Industries, Bohemia, NY, USA). One minute of thorough shaking by hand was performed between the vortexing. The resulting clear suspension was used for dynamic light scattering analysis and ion delivery experiments.

Analysis of the nanodroplet size with dynamic light scattering. The dynamic light scattering was performed on a Microtrac NANO-flex system (Microtrac, York, PA, USA). The refractive index of the dispersed phase was set to 1.33, while the refractive index of the HFE 7500 fluorinated oil was set to 1.29.[25] The viscosity data were obtained from the product information sheet on the 3M website.[26] The set zero time and run time were 60 s and 90 s, respectively, and the number of runs was two.

Generation of alkaline water-in-fluorinated-oil microdroplets and nanodroplet delivery. Water-in-fluorinated microdroplets were generated on a 30 μm fluorophilic chip with the μEncapsulator system from Dolomite Microfluidics (Royston, UK). The disperse phase was the alkaline HEPES buffer (pH 9, 20 mM, NaCl 150 mM), which was loaded into both channels of the sample reservoir chip. The disperse phase was pre-filtered using a 0.22 μm syringe filter (Foxx Life Sciences, Salem, NH, USA). HFE 7500 fluorinated oil containing 2% (w/w) Pico-Surf 1 surfactant was used as the continuous phase. Flow rates of disperse phase in both sample channels and continuous phase were set as 2, 2, and 32 μL/min, respectively. The microdroplets were collected in a 1.5 mL centrifuge tube and stored at room temperature in dark until further processing. The microdroplets can be stored for at least a week at the above condition. To start the reagent delivery, equal volumes of nanodroplets and microdroplets were mixed by gently inverting the tube 5 times. The mixtures were incubated in dark at room temperature.

The microdroplets were inspected using a Leica AF 6000 microscope system with the HC PL FLUOTAR 20×/0.50 DRY and HC PL FLUOTAR 40×/0.80 DRY objective lenses (Wetzlar, Germany). The microdroplet size was analyzed with ImageJ.[27]

Generation of immunosensor-encapsulated microdroplets and nanodroplet delivery. The p53 Quenchbody immunosensor was prepared as described in a previous study.[17] The Quenchbody immunosensor microdroplets were generated on a flow-focusing microfluidic chip with a nozzle size of 20 μm. The disperse phase of 60 nM p53 Quenchbody in PBS buffer (pH 7.4) was loaded into PTFE tubing (inner diameter 0.8 mm) and driven by a syringe pump NE-1000 (New Era, Farmingdale, NY, USA). The HFE 7500 fluorinated oil containing 2% (w/w) FluoSurf surfactant was used as the continuous phase, which was driven by another syringe pump NE-300 (New Era). Flow rates of disperse phase and continuous phase were set as 1 and 4 μL/min, respectively. The nanodroplet preparation was the same as described above with 424 μM human p53 peptide (EPPLSQETFSDLWKLLPENN) (Lifetein, Hillsborough, NJ, USA) solution in PBS. The delivery procedure was the same as described in the previous section.

The microdroplets were observed using an EVOS FL cell imaging system (Thermo Fisher Scientific) with an RFP light cube using Plan Fluorite 20× objective lens at 100% light intensity. The microdroplet size and fluorescence intensity were analyzed with ImageJ. A circular area with a 35-pixel diameter was used for the fluorescence intensity calculation, and the integrated intensity in the red channel was analyzed from three microscopic views of three independent cell counting chambers (Disposable Hemocytometer, Funakoshi, Tokyo, Japan).

Measurement of dose-response curve of p53 Quenchbody. The p53 Quenchbody solution (final concentration, 60 nM) was mixed with different concentrations of human p53 peptide in PBS at 25 °C. The fluorescence intensity of a 60 μL reaction was measured using a CLARIOstar microplate reader (BMG Labtech, Ortenberg, Germany) with excitation and emission wavelengths of 535/20 nm and

585/30 nm (center/bandwidth), respectively. The peptide concentration and the normalized fluorescence intensity were fitted to a four-parameter logistic eqn (1) using ImageJ.

$$y = d + \frac{a-d}{1+\left(\frac{x}{c}\right)^b} \qquad (1)$$

Author Contributions

B.Z. and B.S. conceived the study. B.Z. and Z.D. designed and performed the experiments. Y.D. supported performing the experiments. B.Z. and Z.D. wrote the paper. B.S., S.B., and T.K. provided the resources and supervised the study. All authors discussed the results and edited the manuscript.

Acknowledgments

This work was supported in part by grants from the US National Institute of Health (NIH) AI113406 and GM108703 to B.S., and in part by JSPS KAKENHI Grant Number JP21K14468 from the Japan Society for the Promotion of Science to B.Z. and a Grant-in-Aid for Pioneering Research from Organization for Fundamental Research of Institute of Innovative Research, Tokyo Institute of Technology to B.Z. We thank Dr. James Marti at Minnesota Nano Center for the support on the dynamic light scattering analysis. Portions of this work were conducted in the Minnesota Nano Center, which is supported by the National Science Foundation through the National Nanotechnology Coordinated Infrastructure (NNCI) under Award Number ECCS-2025124.

Conflicts of interest

There are no conflicts to declare.

References

1. D. S. Tawfik and A. D. Griffiths, *Nature biotechnology*, 1998, **16**, 652-656.
2. B. Zhu, T. Mizoguchi, T. Kojima and H. Nakano, *Plos One*, 2015, **10**.
3. A. D. Griffiths and D. S. Tawfik, *The EMBO journal*, 2003, **22**, 24-35.

4. K. Bernath, S. Magdassi and D. S. Tawfik, *Journal of molecular biology*, 2005, **345**, 1015-1026.
5. A. D. Griffiths and D. S. Tawfik, *Trends in biotechnology*, 2006, **24**, 395-402.
6. F. Gielen, R. Hours, S. Emond, M. Fischlechner, U. Schell and F. Hollfelder, *P Natl Acad Sci USA*, 2016, **113**, E7383-E7389.
7. J. Vallapurackal, A. Stucki, A. D. Liang, J. Klehr, P. S. Dittrich and T. R. Ward, *Angew Chem Int Ed Engl*, 2022, **61**, e202207328.
8. D. Vallejo, A. Nikoomanzar, B. M. Paegel and J. C. Chaput, *Acs Synth Biol*, 2019, **8**, 1430-1440.
9. R. Gan, M. D. Cabezas, M. Pan, H. Zhang, G. Hu, L. G. Clark, M. C. Jewett and R. Nicol, *Acs Synth Biol*, 2022, **11**, 2108-2120.
10. E. K. Bowman, J. M. Wagner, S. F. Yuan, M. Deaner, C. M. Palmer, S. D'Oelsnitz, L. Cordova, X. Li, F. F. Craig and H. S. Alper, *P Natl Acad Sci USA*, 2021, **118**.
11. Y. Schaerli and F. Hollfelder, *Mol Biosyst*, 2009, **5**, 1392-1404.
12. C. H. J. Schmitz, A. C. Rowat, S. Koster and D. A. Weitz, *Lab Chip*, 2009, **9**, 44-49.
13. L. M. Fidalgo, C. Abell and W. T. S. Huck, *Lab Chip*, 2007, **7**, 984-986.
14. C. Holtze, A. C. Rowat, J. J. Agresti, J. B. Hutchison, F. E. Angile, C. H. Schmitz, S. Koster, H. Duan, K. J. Humphry, R. A. Scanga, J. S. Johnson, D. Pisignano and D. A. Weitz, *Lab Chip*, 2008, **8**, 1632-1639.
15. J. C. Baret, *Lab Chip*, 2012, **12**, 422-433.
16. K. Okada, R. Ricco, Y. Tokudome, M. J. Styles, A. J. Hill, M. Takahashi and P. Falcaro, *Adv Funct Mater*, 2014, **24**, 1969-1977.
17. Y. C. Dai, Y. Sato, B. Zhu, T. Kitaguchi, H. Kimura, F. J. Ghadessy and H. Ueda, *Chem Sci*, 2022, **13**, 9739-9748.
18. M. Jaiswal, R. Dudhe and P. K. Sharma, *3 Biotech*, 2015, **5**, 123-127.
19. A. Azeem, M. Rizwan, F. J. Ahmad, Z. Iqbal, R. K. Khar, M. Aqil and S. Talegaonkar, *AAPS PharmSciTech*, 2009, **10**, 69-76.

20. A. Gupta, H. B. Eral, T. A. Hatton and P. S. Doyle, *Soft matter*, 2016, **12**, 2826-2841.
21. S. Kishishita, T. Okajima, M. Kim, H. Yamaguchi, S. Hirota, S. Suzuki, S. Kuroda, K. Tanizawa and M. Mure, *J Am Chem Soc*, 2003, **125**, 1041-1055.
22. M. Rolland, N. P. Truong, K. Parkatzidis, E. H. Pilkington, A. L. Torzynski, R. W. Style, E. R. Dufresne and A. Anastasaki, *JACS Au*, 2021, **1**, 1975-1986.
23. K. Bian, F. Chen, Z. T. Humulock, Q. Tang and D. Li, *Chem Res Toxicol*, 2017, **30**, 1794-1796.
24. A. Stucki, P. Juskova, N. Nuti, S. Schmitt and P. S. Dittrich, *Small methods*, 2021, **5**, e2100331.
25. S. K. Tang, Z. Li, A. R. Abate, J. J. Agresti, D. A. Weitz, D. Psaltis and G. M. Whitesides, *Lab Chip*, 2009, **9**, 2767-2771.
26. 3M™ Novec™ 7500 Engineered Fluid, https://multimedia.3m.com/mws/media/65496O/3m-novec-7500-engineered-fluid.pdf, (accessed April 9th, 2023).
27. C. A. Schneider, W. S. Rasband and K. W. Eliceiri, *Nat Methods*, 2012, **9**, 671-675.